Available online at www.sciencedirect.com
SCIENCE DIRECT®
Journal of Nuclear Materials 321 (2003) 256–262
journal of nuclear materials
www.elsevier.com/locate/jnucmat

Control of oxygen concentration in liquid lead and lead–bismuth

G. Müller *, A. Heinzel, G. Schumacher, A. Weisenburger

Forschungszentrum Karlsruhe GmbH, Institute for Pulsed Power and Microwave Technology, P.O. Box 3640, 76021 Karlsruhe, Germany

Received 7 April 2003; accepted 6 May 2003

Abstract

Conditions for control of the oxygen concentration in liquid lead alloys are described using the gas phase as a control medium. Calculation of the Gibbs energy of oxygen in liquid $Pb_{45}Bi_{55}$ is conducted using the data for the binary Pb–O and Bi–O systems. The data obtained are employed to estimate the solubility of oxygen in the $Pb_{45}Bi_{55}$ melt between 200 and 650 °C which is given by $\log c_{O,s}(Pb_{45}Bi_{55}) = 2.52–4803/T$ with T in K. Above 500 °C, agreement is satisfactorily of calculated solubilities with a measurement reported in literature. However, deviations of calculated and measured data increase with decreasing temperatures. Calculated solubilities at 200 °C are 2×10^{-8} wt% compared to 10^{-6} wt% obtained by extrapolation of the measured ones. The obtained solubility data are used to calculate oxygen concentrations at which oxide scales appear that protect steel against dissolution attack by the $Pb_{45}Bi_{55}$ melt without precipitation of PbO. Those concentrations have constant values between 8×10^{-7}–10^{-4} wt% in Pb at 400–600 °C and 4×10^{-10}–10^{-8} wt% in $Pb_{45}Bi_{55}$ at 200–400 °C. These conditions can be established by equilibration with a gas phase containing H_2/H_2O ratios between 10^{-4} and 1.5.

1. Introduction

The proposal of accelerator driven subcritical reactor systems (ADS) with liquid Pb or $Pb_{45}Bi_{55}$ as a coolant and/or target [1] stimulated a number of laboratory work on the compatibility of liquid lead alloys with steel [2–6]. In general the countermeasure against dissolution of steel components by liquid lead alloys is formation of a protective oxide scale on the steel surface which is stabilized by oxygen dissolved in the liquid alloy. This method was first only recently extensively studied and described [7]. The oxide scale hinders cation diffusion from the steel into the liquid metal and vice versa. The chemical activity of oxygen in the lead alloy, however, is a critical parameter, because PbO precipitates if the activity is too high, and steel does not form a protective oxide layer if it is too low [2]. If we consider a liquid metal loop with temperature gradients like in an ADS the situation becomes more complicated because the oxygen partial pressure at which oxide formation occurs varies with temperature. The same happens to the activity of the oxygen dissolved in the lead alloy. Since in a liquid metal loop one has to operate with a constant concentration of oxygen, the relations between concentration, activity and partial pressure of oxygen have to be known.

2. Thermodynamic considerations

The oxygen potential that is required to protect the steel surface by formation of stable oxide layers is here established by control of the H_2/H_2O ratio in the gas atmosphere above the liquid lead alloy. It is known from [7] that the oxygen partial pressure in the gas phase must

* Corresponding author. Tel.: +49-7247 82 4669; fax: +49-7247 82 2256/4874.
E-mail address: georg.mueller@ihm.fzk.de (G. Müller).

0022-3115/$ - see front matter © 2003 Elsevier B.V. All rights reserved.
doi:10.1016/S0022-3115(03)00250-2

be higher than that required for oxidation of iron, the main steel component, and lower than that for PbO formation. Formation of PbO would lead to plugging of the loop. In terms of the Gibbs energies of formation of Fe_3O_4 and PbO this condition is given by

$$2\Delta_f G^\circ(\mathrm{PbO}) > RT \ln p_{O_2} > 0.5\Delta_f G^\circ(\mathrm{Fe_3O_4}), \quad (1)$$

where p_{O_2} gives the oxygen partial pressure in the gas atmosphere in equilibrium with the metal melt. The relation between H_2/H_2O ratio and oxygen partial pressure is given by

$$p_{O_2} = \frac{p^2_{H_2O}}{p^2_{H_2}} \exp\frac{2\Delta_f G^\circ(H_2O)}{RT}. \quad (2)$$

In order to calculate the oxygen concentration c_O in equilibrium with the oxygen partial pressure p_{O_2}, the activity coefficient γ_O has to be known. The activity coefficient can be calculated from the relation for the oxygen activity a_O in Pb and in $Pb_{45}Bi_{55}$ [2],

$$a_O = \gamma_O c_O = \frac{c_O}{c_{O,s}} = \left(\frac{p_{O_2}}{p_{O_2,s}}\right)^{0.5}, \quad (3)$$

assuming the solubility of oxygen $c_{O,s}$ and the corresponding oxygen partial pressure $p_{O_2,s}$ as the standard state. This is a very useful choice of the standard state, because most of the experimental data are obtained for the saturation concentration. Eq. (3) allows to estimate the oxygen activity a_O and the corresponding oxygen partial pressure p_{O_2} if $c_{O,s}$ and $p_{O_2,s}$ are known. With Eq. (3) the activity coefficient amounts to

$$\gamma_O = \frac{1}{c_{O,s}}. \quad (4)$$

Saturation concentrations of oxygen are known from numerous measurements for Pb [8] and for Bi [9] but only from one for the $Pb_{45}Bi_{55}$ melt [10]. The temperature functions for $c_{O,s}$ (wt%) are given by

$$\log c_{O,s}(\mathrm{Pb}) = 1.64 - \frac{3503}{T}, \quad 623 < T(K) < 1323, \quad (5)$$

$$\log c_{O,s}(\mathrm{Bi}) = 2.76 - \frac{4451}{T}, \quad 673 < T(K) < 1323, \quad (6)$$

$$\log c_{O,s}(\mathrm{Pb_{45}Bi_{55}}) = 1.20 - \frac{3400}{T}, \quad (7)$$

where relations (5) and (6) represent fits made by [11] using a data evaluation by Risold et al. [8,9]. The temperature ranges noted to the right of the respective relations show the ranges of the experimental data. This range is not known for the fit in Eq. (7) [10].

The oxygen partial pressure at saturation of oxygen in Pb before PbO precipitation takes place is just given by that over PbO, $RT \ln p_{O_2} = 2\Delta_f G^\circ(\mathrm{PbO})$. Difficulties arise for $Pb_{45}Bi_{55}$ because the partial pressure over $Pb_{45}Bi_{55}$ at saturation concentration of oxygen $c_{O,s}(Pb_{45}Bi_{55})$ is not known. It can be assumed, however, that at the saturation point PbO starts to precipitate and not a mixed $Pb_{45}Bi_{55}$ oxide. But, this will not happen with the same oxygen partial pressure as in the case of pure Pb. It should be calculated.

We calculate partial Gibbs energies of oxygen in $Pb_{45}Bi_{55}$ from those of oxygen in Pb and Bi starting with an approximation proposed by Alcock [12].

$$\Delta\overline{G}^{B}_{A+B+C} = \frac{x_A}{x_A + x_C}\Delta\overline{G}^{B}_{A+B} + \frac{x_C}{x_A + x_C}\Delta\overline{G}^{B}_{C+B} - (1 - x_B)^2\Delta G^{xs}_{A+C}, \quad (8)$$

where $\Delta\overline{G}^{B}_{A+B+C}$ is the partial Gibbs energy of B in a ternary solution of A+B+C with B being the dilute component. Because $x_B \ll 1$ we set $(1 - x_B)^2 = 1$ and get for the $Pb_{45}Bi_{55}$-O system by setting A = Pb, C = Bi and B = O:

$$\Delta\overline{G}_{O_2}(\mathrm{Pb_{45}Bi_{55}[O]}) = x_{Pb}\Delta\overline{G}_{O_2}(\mathrm{Pb[O]}) + x_{Bi}\Delta\overline{G}_{O_2}(\mathrm{Bi[O]}) - 2\Delta G^{xs}(\mathrm{Pb_{45}Bi_{55}}), \quad (9)$$

$\Delta\overline{G}_{O_2}$ = partial Gibbs energy of oxygen, x_{Pb}, x_{Bi} = molar fractions of Pb and Bi, [O] = oxygen in solution, ΔG^{xs} = excess Gibbs energy of mixing of $Pb_{45}Bi_{55}$ (= −1.195 kJ/mol [13]), ΔG^{xs} is given above for 427 °C, but it is assumed to be constant between 200 and 650 °C. This approximation is reasonable, because Pb and Bi form an almost regular solution [11].

The partial Gibbs energy of oxygen dissolved in Pb, $\Delta\overline{G}_{O_2}$ (Pb[O]), and in Bi, $\Delta\overline{G}_{O_2}$ (Bi[O]), can be written as

$$\Delta\overline{G}_{O_2}(\mathrm{Pb[O]}) = 2RT \ln\frac{c_O(\mathrm{Pb})}{c_{O,s}(\mathrm{Pb})} + \Delta\overline{G}_{O_2}(\mathrm{Pb/PbO}), \quad (10)$$

$$\Delta\overline{G}_{O_2}(\mathrm{Bi[O]}) = 2RT \ln\frac{c_O(\mathrm{Bi})}{c_{O,s}(\mathrm{Bi})} + \Delta\overline{G}_{O_2}(\mathrm{Bi/Bi_2O_3}), \quad (11)$$

where c_O is the actual concentration of dissolved oxygen and $c_{O,s}$ its saturation value. The second terms on the right-hand side of Eqs. (10) and (11) concern the partial Gibbs energies of oxygen in the saturated state of the binary systems before PbO or Bi_2O_3 precipitates.

At saturation of oxygen in $Pb_{45}Bi_{55}$, for which PbO starts to precipitate, we get under consideration of the partial excess Gibbs energy of solution of Pb in $Pb_{45}Bi_{55}$

$$\Delta\overline{G}_{O_2}(\mathrm{Pb_{45}Bi_{55}/PbO}) = \Delta\overline{G}_{O_2}(\mathrm{Pb/PbO}) - 2\Delta\overline{G}^{xs}_{Pb}(\mathrm{Pb_{45}Bi_{55}}) = RT \ln p_{O_2,s}(\mathrm{Pb_{45}Bi_{55}}), \quad (12)$$

where in this case we have to use the partial excess Gibbs energy of mixing Pb into $Pb_{45}Bi_{55}$ (1.59 kJ/mol [13])

because we refer now to the equilibrium of the $Pb_{45}Bi_{55}$ melt with PbO. It shows that PbO precipitation takes place at a higher oxygen potential in $Pb_{45}Bi_{55}$ because $\Delta\overline{G}^{xs}_{Pb}(Pb_{45}Bi_{55}) < 0$. If we set now $\Delta\overline{G}_{O_2}(Pb_{45}Bi_{55}[O]) = \Delta\overline{G}_{O_2}(Pb_{45}Bi_{55}/PbO)$ and $c_O(Pb) = c_O(Bi) = c_{O,s} \times (Pb_{45}Bi_{55})$, assuming the saturated state, we arrive in combining Eqs. (9)–(12) at

$$C_{O,s}(Pb_{45}Bi_{55}) = C_{O,s}(Pb)^{x_{Pb}} C_{O,s}(Bi)^{x_{Bi}} \cdot \exp\frac{x_{Bi}(2\Delta_f G^\circ(PbO) - \frac{2}{3}\Delta_f G^\circ(Bi_2O_3))}{2RT}, \quad (13)$$

where we replaced the partial Gibbs energies of oxygen of the saturated Pb and Bi melts by the Gibbs energies of formation of PbO and Bi_2O_3, and set for simplicity of Eq. (13) $\Delta G^{xs}(Pb_{45}Bi_{55}) = \Delta\overline{G}^{xs}_{Pb}(Pb_{45}Bi_{55})$. This latter approximation has practically no influence on the result of the calculation with Eq. (13).

The saturation concentration calculated is drawn in Fig. 1 as a function of temperature together with those for the Pb, Bi and $Pb_{45}Bi_{55}$ melts [10] according to Eqs. (5)–(7). Looking at the diagram we have to keep in mind the large scatter of Pb data in [8] at low temperatures and their extrapolation to temperatures below the melting point. This, however, cannot be the only reason for the large deviation between the calculated data and those obtained by measurements (Eq. (7)). Therefore, it is obviously necessary to confirm by additional measurements how the temperature function of $c_{O,s}$ looks especially at lower temperatures.

If we fit the curve for $c_{O,s}(Pb_{45}Bi_{55})$ calculated with Eq. (12) using a function like those in Eqs. (5)–(7) we arrive at

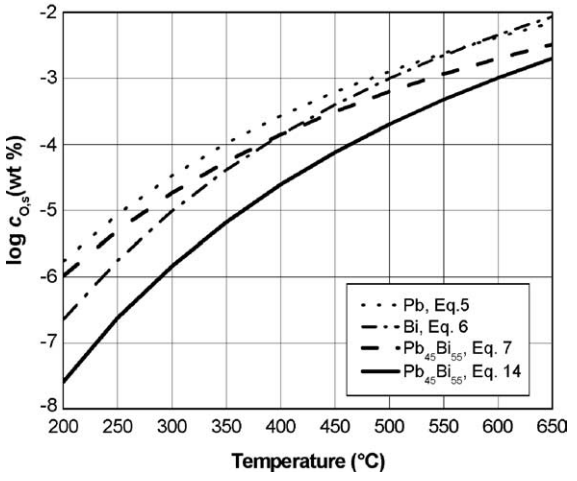

Fig. 1. Oxygen solubilities in Pb and Bi according to a fit of data collected by Risold [8,9] and in $Pb_{45}Bi_{55}$ (Eq. (7)) obtained by Gromov [10] and Eq. (14) according to our calculations.

$$\log c_{O,s}(Pb_{45}Bi_{55}) = 2.52 - \frac{4803}{T}, \quad (14)$$

where $c_{O,s}(Pb_{45}Bi_{55})$ is given in wt%.

Knowing the saturation concentration we can now write the concentration dependence of $\Delta\overline{G}_{O_2}$ for the $Pb_{45}Bi_{55}$ melt.

$$\Delta\overline{G}_{O_2}(Pb_{45}Bi_{55}[O]) = 2RT\ln\frac{c_O(Pb_{45}Bi_{55})}{c_{O,s}(Pb_{45}Bi_{55})} + 2\Delta_f G^\circ(PbO) - 2\Delta\overline{G}^{xs}_{Pb}(Pb_{45}Bi_{55}) \quad (15)$$

and use this equation for determination of the Gibbs energy of oxygen dissolved in $Pb_{45}Bi_{55}$ and its partial pressure above the melt. For saturation conditions the logarithmic term gets zero and we arrive at Eq. (12) again.

3. The principle of oxygen control via the gas phase

It is not possible to use an oxygen/inert gas mixture, e.g. O_2/Ar, to control the oxygen concentration in the liquid metal because the oxygen partial pressure would be too low ($<10^{-15}$ bar) to deliver the oxygen consumed by oxide scale formation on steel structures. Therefore, a mixture of H_2 and H_2O is used to control the concentration of oxygen in the liquid metal. It allows to carry a sufficient amount of oxygen at an oxygen partial pressure that corresponds to the stability conditions given in Eq. (1).

The diagram in Fig. 2 demonstrates in which region the stable conditions exist and how they can be established. The ordinate shows the partial Gibbs energy of oxygen expressed by the oxygen partial pressure, the abscissa the temperature. The lines of constant H_2/H_2O ratios and those of constant oxygen partial pressures, P_{O_2}, show the ratios which must be established in the gas phase to attain a certain oxygen partial pressure. Those lines intersect at absolute zero temperature, the P_{O_2} lines at $RT\ln p_{O_2} = 0$ and the H_2/H_2O lines at $RT\ln p_{O_2} = 2\Delta_f G^\circ$ (H_2O). The important region with protective oxide scale formation is the one between the lines for PbO and Fe_3O_4/FeO in the temperature region of 200–650 °C, which is relevant for loops with liquid $Pb_{45}Bi_{55}$ and Pb.

The diagram also contains lines of constant oxygen concentration in Pb and the $Pb_{45}Bi_{55}$ melt in equilibrium with the corresponding oxygen partial pressure and H_2/H_2O ratios. The lines for Pb are calculated using Eqs. (5) and (10), those for the $Pb_{45}Bi_{55}$ melt from Eqs. (14) and (15). First ones end at the melting point. We note three different properties of the curves in Fig. 2. Gibbs energies are higher for oxygen in the $Pb_{45}Bi_{55}$ melt than for Pb at the same oxygen concentration. The slope of the concentration of oxygen with increasing temperature is steeper for the $Pb_{45}Bi_{55}$ melt than for Pb. The curve for the partial Gibbs energy of oxygen in the saturated $Pb_{45}Bi_{55}$ melt appears about 3 kJ/mol above that for the pure Pb melt.

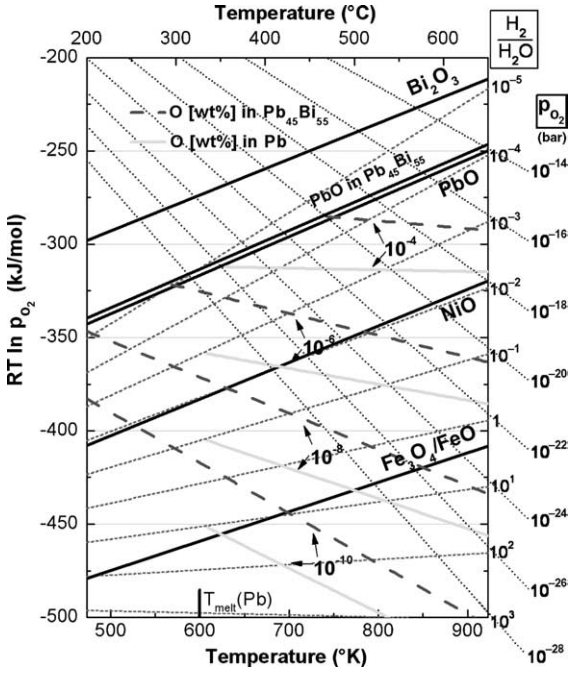

Fig. 2. Ellingham–Richardson diagram containing oxides of steel components and of Bi and Pb. Lines of constant oxygen concentrations in Pb and the $Pb_{45}Bi_{55}$ melt indicate the stability regions of iron oxide without PbO precipitation in the temperature gradient of a loop.

Since the liquid metal containing a defined oxygen concentration extends over regions with about 150 and 200 °C temperature differences in a liquid metal loop, it is most convenient to use c_O/T diagrams for determination of the stability ranges of steel in Pb and the $Pb_{45}Bi_{55}$ melt. The first diagram (Fig. 3) shows the situation in a Pb loop over a temperature range from the melting point to 650 °C. Two boundary curves enclose the limits of the stability range given by Eq. (1).

The upper curve is $c_{O,s}(Pb)(T)$ and the lower $c_O(Fe_3O_4/FeO)(T)$ which is the equilibrium concentration of oxygen in the $Pb_{45}Bi_{55}$ melt in contact with Fe/Fe_3O_4 or with Fe/FeO above 570 °C. For oxygen control in a temperature region between 400 and 600 °C we select the shaded area and end up with a concentration range of 8×10^{-7}–10^{-4} wt% of oxygen. This concentration is easily controlled by a H_2/H_2O ratio of 0.38–3×10^{-3} at 600 °C that can be calculated from the dissociation equilibrium of water vapor.

We obtain from Eqs. (2) and (3):

$$\frac{p_{H_2}}{p_{H_2O}} = \frac{c_{O,s}}{c_O\sqrt{p_{O_2,s}}} \exp\left(\frac{\Delta_f G^\circ(H_2O)}{RT}\right) \tag{16}$$

or

$$\frac{p_{H_2}}{p_{H_2O}} = \frac{c_{O,s}}{c_O} \exp\left(\frac{\Delta_f G^\circ(H_2O) - \Delta_f G^\circ(PbO)}{RT}\right). \tag{17}$$

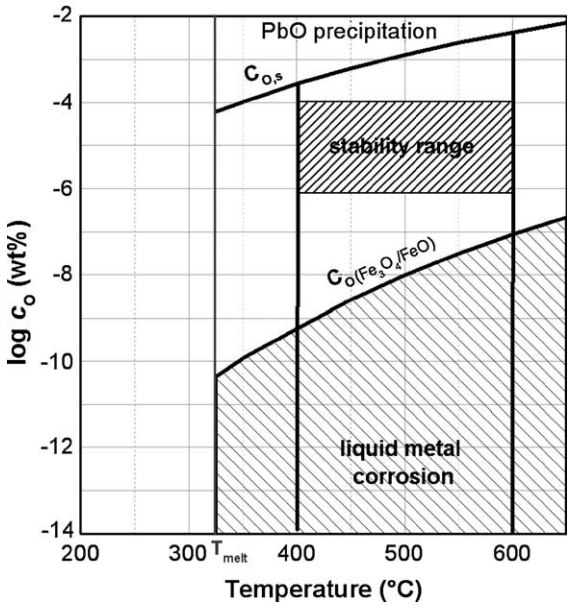

Fig. 3. Range between the solubility limit $c_{O,s}$ and the oxygen concentration at which decomposition of iron oxides takes place. The area between the curves indicate the concentrations for which stable conditions are expected in a loop with liquid Pb.

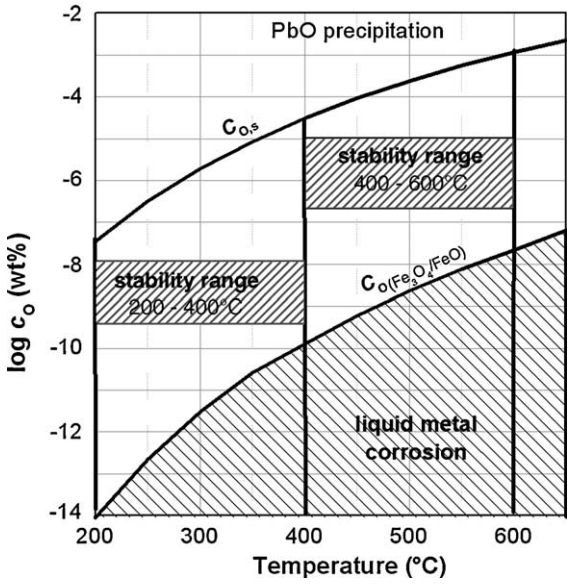

Fig. 4. Range between the solubility limit $c_{O,s}$ and the oxygen concentration at which decomposition of iron oxides takes place. The area between the curves indicate the concentrations for which stable conditions are expected in a loop with the $Pb_{45}Bi_{55}$ melt.

In case of the $Pb_{45}Bi_{55}$ melt the curves differ from those for the Pb melt because of the different saturation concentrations and the contribution of ΔG^{xs} ($Pb_{45}Bi_{55}$) described in Eq. (9). Fig. 4 shows the situation in a

$Pb_{45}Bi_{55}$ melt in which the lowest loop temperature could be around 200 °C.

For the calculations we took Eq. (14) for $c_{O,s}(Pb_{45}Bi_{55})$ and Eq. (15) for $c_O(Fe_3O_4/FeO)$, the latter one by setting $\Delta\overline{G}_{O_2}(Pb_{45}Bi_{55}[O]) = \frac{1}{2}\Delta_f G°(Fe_3O_4/\ 4FeO)$.

If we look at the low temperature region between 200 and 400 °C, a working range of 4×10^{-10} and 10^{-8} wt% can be defined corresponding to H_2/H_2O ratios of 0.9–3.6×10^{-2} at 400 °C. Between 400 and 600 °C the corresponding range would be between 2×10^{-7} and 10^{-5} wt% of oxygen with H_2/H_2O ratios of 0.26–5.2×10^{-3} at 600 °C. The equilibrium H_2/H_2O ratios are calculated by combining Eq. (12) with Eq. (16) as follows:

$$\frac{p_{H_2}}{p_{H_2O}} = \frac{c_{O,s}(Pb_{45}Bi_{55})}{c_O} \times \exp\left(\frac{\Delta_f G°(H_2O) - \Delta_f G°(PbO) + \Delta\overline{G}^{xs}_{Pb}(Pb_{45}Bi_{55})}{RT}\right). \quad (18)$$

4. Oxygen control system

The gases Ar and Ar/5%H_2 are mixed in an oxygen control system by two flow controllers to obtain the required hydrogen concentration in the cover gas, Fig. 5. The gas passes through a moisturizer, the water vapour pressure of which is controlled by a precision thermostat. The oxygen control by equilibration between gas phase and liquid metal in the reaction tube is sketched in the shaded area of Fig. 5. The incoming and outcoming gas is checked by a moisture sensor and finally by an oxygen partial pressure detector. The used moisture sensor is a dew point meter DEWMET SD from MICHELL, the partial pressure detector a SGMT 1.1 from ZIROX.

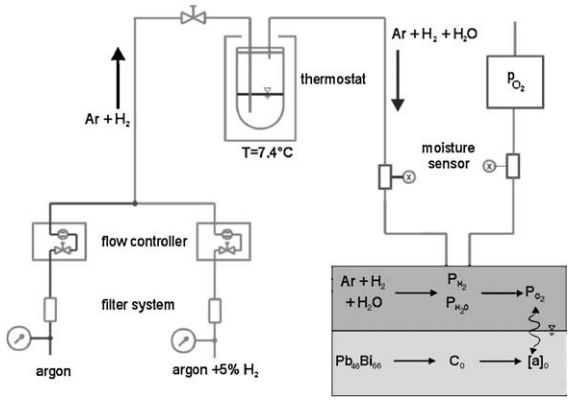

Fig. 5. Scheme of an oxygen control system with gas conditioning and control. The shaded areas show the equilibrium processes taking place between gas phase and the $Pb_{45}Bi_{55}$ melt.

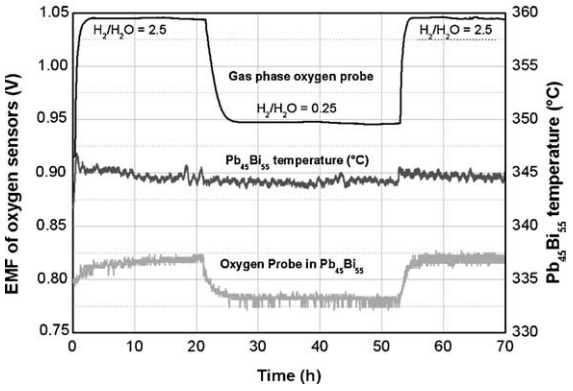

Fig. 6. Equilibration of oxygen activities between the gas phase and the $Pb_{45}Bi_{55}$ melt in a liquid metal loop.

On the principle described above, the oxygen control system was developed and build to control the oxygen concentration in the KALLA loops at FZK. The oxygen control of 1000 l of $Pb_{45}Bi_{55}$ inventory is accomplished under flow conditions in this loops. The surface that is exposed to the control gas flow is about 0.14 m^2 at a temperature of 345 °C.

The time scale in which the equilibration of the oxygen activity between the gas phase and the liquid metal is reached in the loop is demonstrated in Fig. 6 by comparison of the EMF signals of the zirconia oxygen sensors in the gas phase and in the liquid metal.

The oxygen activity in the $Pb_{45}Bi_{55}$ melt, represented by the EMF signal of the Pt/air oxygen meter in the lower curve, follows quite closely that of the oxygen partial pressure change in the gas phase. This latter one is depicted by the signal of the gas oxygen meter in the upper curve. It takes only about 5 h at 345 °C to establish the new oxygen activity in $Pb_{45}Bi_{55}$ that corresponds to the new H_2/H_2O ratio of 0.25. The reverse process, i.e. the reduction of the activity to the initial value at a H_2/H_2O ratio of 2.5 took only about half of the time. The difference can be explained by considering the hydrogen that gets dissolved in the liquid metal.

In any case, the experiment shows that the response of the oxygen activity in the liquid metal loop to changes in the gas phase is fast enough to allow an oxygen control via the gas phase also in large loops.

5. Discussion

Control of oxygen concentration in liquid Pb and eutectic $Pb_{45}Bi_{55}$ melt through the gas phase requires knowledge of the relation between the oxygen partial pressure in the gas phase and the oxygen concentration in the liquid metal or metal alloy. Instead of using the oxygen activity in the liquid metal as a control para-

meter it is more convenient to take the oxygen concentration because this one remains constant throughout the whole temperature range existing in a liquid metal loop. In any case, the oxygen solubility in the liquid metal must be known as a function of temperature, because this concentration determines the highest value of the Gibbs energy of oxygen that can be tolerated in a loop to prevent precipitation of PbO in low temperature regions.

Calculation of the Gibbs energy of oxygen in the eutectic $Pb_{45}Bi_{55}$ melt from data of the Pb–O and Bi–O binary systems shows that it is higher for the $Pb_{45}Bi_{55}$ melt by about 20–30 kJ/mol than that in Pb for the same oxygen concentration. Furthermore, the solubility limit of oxygen in $Pb_{45}Bi_{55}$ is lower than that in liquid Pb. This leads to the fact that the oxygen partial pressure in the gas phase must be about two orders of magnitude higher above the $Pb_{45}Bi_{55}$ melt as compared to the Pb melt to achieve the same oxygen concentration (see Fig. 2). Considering this difference we have to keep in mind that not only the Gibbs energy but also a high enough concentration of oxygen in the liquid metal is responsible for formation of a protective oxygen scale on the steel surface.

Knowing the relation between the Gibbs energy of oxygen and the oxygen concentration in a liquid alloy, it is possible to calculate the saturation concentration of oxygen in the $Pb_{45}Bi_{55}$ melt. This is done by assuming that PbO starts to precipitate at the saturation point. As shown in Fig. 1 the calculated solubilities agree satisfactorily at high temperatures with those measured by Gromov et al. [10], but the deviation gets larger with decreasing temperatures and reaches a factor of 30 at 200 °C. By now it is not possible to give an explanation for this difference. But, it must be assumed that the measurements were done at higher temperatures, probably above 400 °C, and the main difference is caused by the extrapolation of the data to low temperatures using Eq. (7). The data calculated using Eq. (13) base on thermodynamic functions and may give a better extrapolation down to low temperatures. However, we have to consider that data of the oxygen solubility in Pb used in Eq. (13) are extrapolated with Eq. (5) down to 200 °C beyond the melting point of Pb. This seems to be a reasonable approximation because the Pb component in the eutectic $Pb_{45}Bi_{55}$ alloy stays liquid down to this temperature. What are now the consequences of the difference between measured and calculated solubilities of oxygen? In Fig. 7, the $c_O(T)$ functions are shown using the two data sets for the oxygen concentration at saturation (upper pair of curves) and at Fe_3O_4/FeO decomposition (lower curves).

We see that for temperature differences of 150–200 °C, as expected for liquid metal loops, it is easily possible to define concentration regions in which the stability criteria are satisfied for both data sets, the measured and calculated ones. However, for temperature differences that extend over the whole diagram up to 650 °C we run into difficulties. If we equilibrate with an oxygen concentration of 2×10^{-8} wt% at 200 °C, just at the saturation point given by the calculated curve, we will run into Fe_3O_4/FeO decomposition at 650 °C. Now, there is not such a large temperature difference expected to be in a liquid metal loop. However, in some laboratories, the saturation concentration in a tank at 200 °C is used to establish the oxygen concentration for experiments at 600–650 °C. In this case it is important to know the exact course of $c_{O,s}(T)$ at low temperatures. If the calculated curve is the right one, saturation equilibration has to be established at 300 °C to achieve an oxygen concentration of 10^{-6} wt% at 650 °C. Equilibration at 200 °C would lead to an oxygen concentration of 2×10^{-8} wt% and to decomposition of Fe_3O_4/FeO at the high temperatures. It is necessary, therefore, to conduct further solubility measurements for oxygen in the $Pb_{45}Bi_{55}$ melt especially at low temperatures. One has to pay attention to reaction processes that appear in experiments involving large temperature differences.

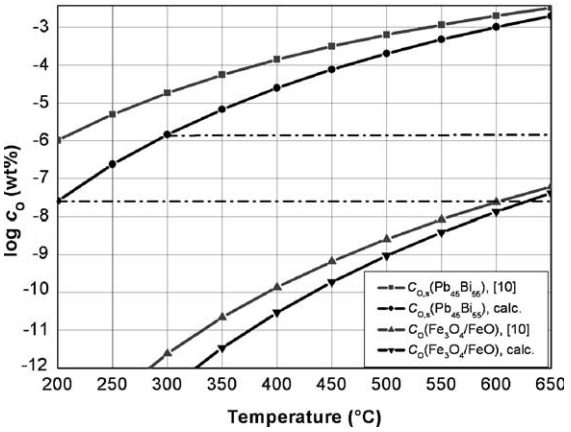

Fig. 7. Comparison of stability ranges enclosed between curves according to experimental data [10] and those obtained by calculation with Eq. (14).

6. Conclusion

Calculation of Gibbs energies of oxygen as a function of its concentration in the liquid, eutectic $Pb_{45}Bi_{55}$ alloy reveal that two orders of magnitude higher oxygen partial pressures over the $Pb_{45}Bi_{55}$ melt than over the Pb melt must be established to achieve the same oxygen concentration in the alloy. When this function is used to calculate oxygen solubility data in eutectic $Pb_{45}Bi_{55}$, the agreement with data of the only known measurement is satisfactorily at temperatures above 500 °C. Below 500 °C, discrepancies get larger with decreasing temperatures. Since not many details are known about the

available experimental data one has to keep in mind that the oxygen solubility at 200 °C could be as well more than one order of magnitude lower. This has implications on experiments employing large temperature differences. Measurements of the oxygen solubility in eutectic $Pb_{45}Bi_{55}$ are necessary, especially for temperatures below 500 °C. It is shown that stability ranges for concentration control through the gas phase in loops can be defined considering both data sets.

The oxygen control of $Pb_{45}Bi_{55}$ in loops is demonstrated. It is shown that equilibration between gas phase and liquid $Pb_{45}Bi_{55}$ is fast enough for the control of oxygen concentration in $Pb_{45}Bi_{55}$.

Acknowledgements

The work has been performed in the frame work of the Nuclear Safety Program of the Research Center Karlsruhe. The authors like to thank Mr C.H. Lefhalm for the measurement of oxygen activities in the THESYS loop at KALLA laboratory.

References

[1] C. Rubbia, J.A. Rubio, S. Buono, F. Carminati, Conceptual Design of a Fast Neutron Operated High Power Energy Amplifier, CERN/AT/95-44 (ET), 29 September 1995.
[2] G. Müller, G. Schumacher, F. Zimmermann, J. Nucl. Mater. 278 (2000) 85.
[3] G. Benamati, P. Buttol, V. Imbeni, C. Martini, G. Palombarini, J. Nucl. Mater. 278 (2000) 308.
[4] G. Müller, A. Heinzel, J. Konys, G. Schumacher, A. Weisenburger, F. Zimmermann, V. Engelko, A. Rusanov, V. Markov, J. Nucl. Mater. 301 (2002) 40.
[5] F. Barbier, A. Rusanov, J. Nucl. Mater. 296 (2001) 231.
[6] L. Soler Crespo, F.J. Martín Munoz, D. Gómez Briceno, J. Nucl. Mater. 296 (2001) 273.
[7] B.F. Gromov, Yu.I. Orlov, P.N. Martynov, K.D. Ivanov, V.A. Gulevski, in: H.U. Borgstedt, G. Frees (Eds.), Liquid Metal Systems, Plenum, NY, 1995, p. 339.
[8] D. Risold, B. Hallstedt, L.J. Gaukler, H.L. Lukas, S.G. Fries, J. Phase Equil. 16 (1995) 223.
[9] D. Risold, J.I. Nagata, R.O. Suzuki, J. Phase Equil. 19 (1998) 213.
[10] F. Gromov, Yu.I. Orlov, P.N. Martynov, V.A. Gulevski, Proceedings of the Conference HLMC 98, Obninsk: SSC RF–IPPE, vol. 1, 1999, p. 83.
[11] A. Heinzel, Dissertation Uni Karlsruhe 2002, report FZKA 6823, 2003.
[12] C.B. Alcock, in: G.R. Fitterer (Ed.), Application of Fundamental Thermodynamics to Metallurgical Processes Proceedings, Gordon and Breach, NY, 1967, p. 39.
[13] R. Hultgren, P.D. Desai, D.T. Hawkins, M. Geiser, K.K. Kelly, Selected values of the thermodynamic properties of binary alloys, Am. Soc. Met., Metals Park, Ohio 44073, 1973, p. 443.